

Two-dimensional photonic crystals with Ge/Si self-assembled islands

S. David, M. El kurdi, P. Boucaud,^{a)} A. Chelnokov,^{b)} V. Le Thanh,^{c)} D. Bouchier, and J.-M. Lourtioz

Institut d'Electronique Fondamentale, UMR CNRS 8622, Bâtiment 220, Université Paris-Sud, 91405 Orsay, France

(Received 16 January 2003; accepted 23 July 2003)

Two-dimensional photonic crystals were fabricated on silicon-on-insulator waveguides with self-assembled Ge/Si islands deposited on top of the upper silicon layer. The photonic crystals consist of triangular lattices of air holes designed to exhibit a forbidden band around $1.5\ \mu\text{m}$. Different hexagonal photonic crystal microcavities were processed whose optical properties are probed at room temperature with the Ge/Si island photoluminescence. Quality factors larger than 200 are measured for hexagonal H3 cavities. A significant enhancement of the Ge/Si island photoluminescence is achieved in the $1.3\text{--}1.55\ \mu\text{m}$ spectral region using the photonic crystal microcavities. We show that the energy resonance of the defect modes can be tuned with the filling factor of the photonic crystal. © 2003 American Institute of Physics. [DOI: 10.1063/1.1612892]

Thin slabs of two-dimensional (2D) photonic crystals (PC) can modify the radiation pattern of spontaneous emission by changing the density of optical modes at the transition frequency.¹ Strong light extraction efficiency from semiconductor slab waveguides was obtained owing to the coherent scattering of the internally trapped spontaneous emission and its coupling to the leaky modes above the light line.² Alternatively, the presence of point defects acting as microcavities in 2D PC slabs can also improve the light extraction from micro (nano)-emitters since they offer high quality factors and small mode volumes. For instance, an enhanced light emission from InGaAs quantum dots in a two-dimensional PC microcavity was recently reported.³ In turn, the optical properties of photonic crystals and microcavities themselves can be probed by inserting layers of self-assembled quantum dots as active emitters in the structure.⁴ High quality factors in excess of 1000 were measured in PC membranes with III–V materials by using this method.⁵ Highly localized donor modes resonances with narrow linewidth were observed in single defect slab cavities fabricated on an AlO_x layer.⁶

Although the association of 2D PC microcavities with self-assembled micro (nano)-emitters can be repeated in a large variety of materials, there is no report of such an experiment in silicon-based materials. Two-dimensional photonic crystals etched in a silicon-on-insulator (SOI) waveguide were recently demonstrated with a forbidden band around $1.5\ \mu\text{m}$.⁷ Indeed, the availability of the SOI substrates on a large scale together with a strong optical confinement provided by a high refractive index contrast between silicon and silica ($\Delta n \sim 2$) are true advantages for the development of silicon-based microphotonic. Besides, the insertion of active emitters operating in the 1.3 and $1.55\ \mu\text{m}$ spectral regions can be achieved by growing Ge/Si self-assembled islands on top of the SOI substrate.⁸ The growth of Ge/Si self-

assembled islands offers several advantages: (i) the islands emit at long wavelength ($1.3\text{--}1.55\ \mu\text{m}$) in the transparency window of the silicon matrix. (ii) the islands can be easily integrated in silicon-based processes and remain fully compatible with metal–oxide–semiconductor processes. The compatibility of structures combining Ge/Si islands and photonic crystals with silicon-based processes represents an intrinsic advantage as compared to the heterogeneous report of III–V materials on silicon for the development of light emitters. These structures can also be coupled with microphotonic devices processed on a silicon platform.

In this letter, we report a study of two-dimensional photonic crystal microcavities on silicon-on-insulator waveguides with self-assembled Ge/Si quantum islands deposited on top of the upper crystalline silicon layer. The vertical confinement of light is provided by the silicon-Ge/Si guiding multilayers. The lateral confinement is created by the two-dimensional crystal obtained by drilling arrays of air holes in the top silicon layer. The photonic crystal slab contains three layers of Ge/Si self-assembled islands grown by chemical vapor deposition using a Stranski–Krastanow growth mode. Several hexagonal defect cavities are processed by electron beam lithography by omitting to drill some holes. The photonic crystal optical properties are investigated at room temperature using the Ge/Si island photoluminescence in a normal incidence geometry. We show that the microcavity modes can be probed in the spectral region around $1.3\text{--}1.55\ \mu\text{m}$. A significant enhancement of the photoluminescence is observed with these PC microcavities whose resonances can be tuned by adjusting the filling factor of the photonic crystals.

In the experiments, the studied samples were grown on SOI substrates with a $3.5\text{-}\mu\text{m}$ -thick buried oxide layer and a $0.2\text{-}\mu\text{m}$ -thick silicon layer lying on top of the oxide. The active layer consisting of three Ge/Si self-assembled island layers separated by $20\ \text{nm}$ silicon barriers was grown by low pressure chemical vapor deposition.⁹ The islands had a typical base width of $120\ \text{nm}$ and an height of $10\ \text{nm}$. The island density was around $1 \times 10^9\ \text{cm}^{-2}$. The vertical correlation of the islands was observed by cross-section transmission

^{a)}Electronic mail: philippe.boucaud@ief.u-psud.fr

^{b)}Present address: Corning SA, 77210 Avon, France.

^{c)}Present address: Centre de Recherche sur les Mécanismes de la Croissance Cristalline, CRMC2-CNRS, Campus de Luminy, Case 913, 13009 Marseille, France.

electron microscopy. At room temperature, the island photoluminescence measured on PC free regions of the samples is resonant around 0.91 eV with a full width at half maximum of 0.11 eV. The total thickness of the waveguide core including Ge/Si island layers was 0.3 μm . This value is sufficiently small to ensure single-mode waveguiding at 1.5 μm once the whole PC structure was processed. After the island growth, a 0.2- μm -thick oxide layer was deposited on top to provide an hard mask for silicon etching. The 2D PC and microcavities were defined by electron beam lithography. Triangular lattices of holes with a 0.5 μm period were then processed. The hole diameter was varied by modifying the electron dose. The pattern was transferred successively into the oxide layer and the guiding silicon-Ge/Si multilayers using reactive ion etching. The oxide layer and guiding silicon-Ge/Si multilayers were etched with CHF_3 and SF_6 gases, respectively. The whole patterned surface was $50 \times 50 \mu\text{m}^2$. The holes drilled into the silicon-Ge/Si multilayers down to the buried oxide layer had diameters between 0.3 and 0.45 μm . Correspondingly, the air filling factor of the photonic crystals was between 23% and 81%. Different hexagonal cavities (H2–H3 and H5) were defined in the photonic crystal.¹⁰ After etching the holes, a thin oxide layer of the hard mask was kept on top of the structure, thus lowering the waveguide asymmetry. The photoluminescence was measured at room temperature with an Ar^+ pump laser beam in a normal incidence configuration. The excitation and photoluminescence beams were focused and collected with the same objective of 0.65 numerical aperture. The excitation power was ~ 20 mW focused on a $\sim 2 \mu\text{m}$ spot diameter. The luminescence was filtered with a 100 μm diameter pinhole located at the focal point of a 15 cm focal lens. The luminescence was dispersed by a monochromator and detected with a liquid-nitrogen cooled germanium detector using standard lock-in techniques. The alignment of the pump beam on the cavity axis was achieved by imaging the sample surface with the argon laser.

Figure 1(a) shows a scanning electron micrograph of the 2D triangular lattice PC with a H3 cavity. Figure 1(b) shows a schematic cross section of the structure. The lattice period a is 500 nm, corresponding to a normalized frequency $a/\lambda = 0.32$ at 1.55 μm . The hole diameter is 0.4 μm . The hole diameter is adjusted to tune the photonic gap not far from 1.5 μm .

Figure 2 shows the band structure of the two-dimensional triangular lattice for the TE polarization. The calculations were performed using a plane wave method with an interhole spacing of 0.5 μm and a hole radius of 0.2 μm . The effective indexes used in the calculations were adapted to fit the results obtained below the light line with a three-dimensional plane wave model.¹¹ Note that the sole three-dimensional plane wave model is not valid for the modes above the light line. It explains why we used a two-dimensional calculation with a fit of the effective indexes obtained with the three-dimensional calculation below the light line. The inset of Fig. 2 shows the first Brillouin zone and the symmetry directions in the k space over which the calculations are performed. The light line associated with the oxide cladding given by the dispersion relation $\omega = ck_x/n_{\text{cladding}}$ is depicted as an oblique dashed line. No

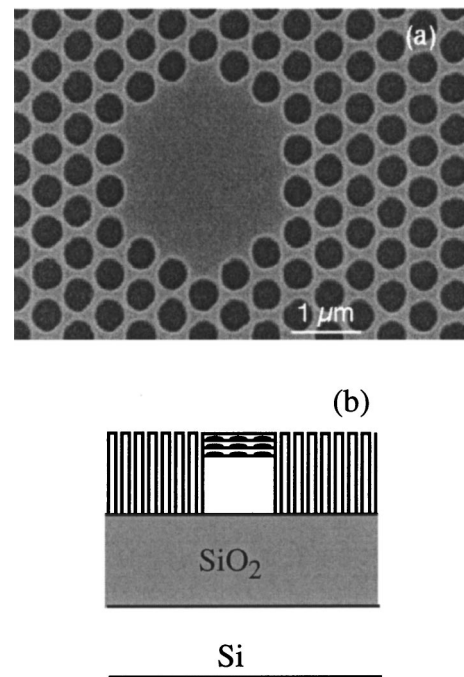


FIG. 1. (a) Scanning electron micrograph of a photonic crystal H3 cavity fabricated on a silicon-on-insulator substrate. The hole spacing is 0.5 μm . The hole diameter is $\sim 0.4 \mu\text{m}$. (b) Schematic cross section of the structure.

mode can propagate into the air below the light line. In contrast, the optical modes can be coupled to the continuum of radiative modes above the light line. The calculated in-plane photonic band gap for a TE polarization extends from 0.66 to 1.03 eV. No band gap exists for a TM polarization. The band gap spectral width varies from 0.42 to 0.3 eV when the hole radius is decreased from 0.225 to 0.175 μm . As will be shown later, the emission of the Ge/Si islands is resonant around 0.9 eV at room temperature and can be detected between 0.8 and 1.03 eV. The emission of silicon can be detected between 1.030 and 1.15 eV with a resonance around 1.07 eV. The active emitters inside the photonic crystals have thus spectral distributions which cover a large fraction of the forbidden gap. The defect modes calculated for a H2 cavity using a supercell approach are represented by the horizontal

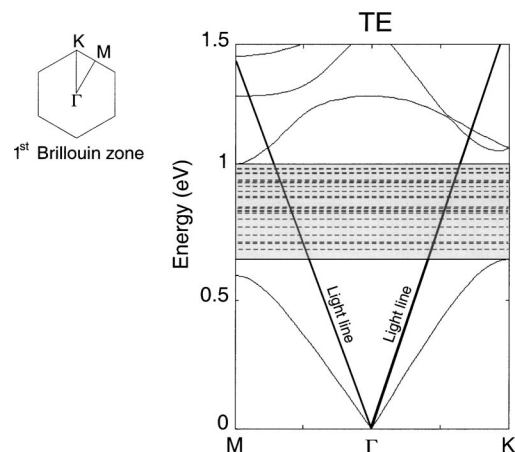


FIG. 2. Calculated dispersion diagram of the photonic structure. The gray area corresponds to the photonic band gap. The diagram on the left shows the symmetry directions of the first Brillouin zone over which the calculations are performed. The defect modes of a H2 cavity appear as horizontal dashed lines in the gap. The light lines are represented by oblique lines in the diagram.

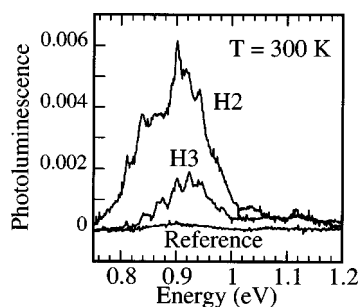


FIG. 3. Room temperature photoluminescence of H2 (top curve) and H3 cavities (bottom curve) compared to the photoluminescence of the sample measured outside of the photonic crystal. The hole diameter is $0.2 \mu\text{m}$. The vertical scale is identical for the three spectra.

dashed lines in Fig. 2. The parameters used to calculate the defect modes are the same as those used to compute the two-dimensional photonic band gap. The number of confined modes in the band gap is equal to 22 for the H2 cavity.

Figure 3 shows the photoluminescence spectra of H2 and H3 cavities compared to the photoluminescence of the structure recorded outside the photonic crystals. The hole radius of the photonic crystal is $0.2 \mu\text{m}$. The presence of the cavity leads to the appearance of multiple resonances that modulate the photoluminescence spectra. These resonances correspond to the cavity modes that are coupled to the leaky continuum modes. A significant enhancement of the room temperature photoluminescence is observed as the cavity size is decreased. We also found that the photoluminescence signal amplitude was superlinear as a function of the pump excitation density in the case of the small cavities. A detailed analysis of this effect is beyond the scope of this letter and will be published elsewhere.¹² A $\times 30$ enhancement is presently observed for the H2 cavity around 0.9 eV as compared to the reference. This comes with a spectral broadening of the detected signal. The integrated emitted power of the H2 microcavity is around 400 nW at room temperature. A significant emission can now be detected at $1.55 \mu\text{m}$ while no emission could be detected at this wavelength in the unprocessed sample under the same excitation conditions. Indeed, this result shows the great potential of two-dimensional photonic crystal microcavities associated to Ge/Si self-assembled islands to enhance the light emission around $1.55 \mu\text{m}$ in silicon-based devices.

Figure 4 shows a comparison of the room temperature photoluminescence spectra of H3 cavities for two different hole radius. The top curve corresponds to a $0.175 \mu\text{m}$ hole radius while the bottom curve corresponds to a $0.2 \mu\text{m}$ hole radius. An enhancement of the emission is clearly observed as the hole radius is increased. Larger holes *a priori* lead to a better coupling to the radiative modes above the light line. However, further work will be required to quantify this feature. The change of the hole radius also leads to an energy shift of the resonant emission. For a $0.175 \mu\text{m}$ hole radius, a resonant mode is observed at 0.801 eV (i.e., $1.548 \mu\text{m}$) in the spectral region of the telecommunication wavelengths. The narrowest resonances are observed at the longest wavelength around 0.81 eV . The quality factor of these modes, defined as $Q = \omega/\Delta\omega$, is around 220. The Q values of the cavity modes are lower at shorter wavelengths. This feature is explained by

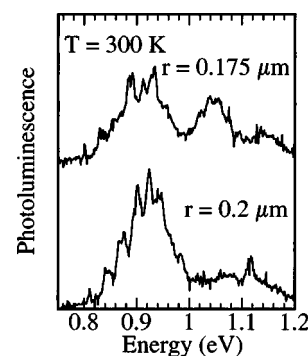


FIG. 4. Room temperature photoluminescence of a H3 cavity for two different hole radii: $0.175 \mu\text{m}$ (top curve) and $0.2 \mu\text{m}$ (bottom curve). The hole spacing is $0.5 \mu\text{m}$. The upper curve has been shifted for clarity. The same vertical scale is used for the two curves.

the simultaneous increase of the radiation losses and material absorption at shorter wavelengths.¹³

In conclusion, we have fabricated two-dimensional photonic crystals on silicon-on-insulator substrates. Ge/Si self-assembled islands have been incorporated inside the crystals as active emitters. The island emission at room temperature was used to probe the properties of photonic crystal microcavities. Quality factors larger than 200 have been measured near $1.55 \mu\text{m}$ for H3 hexagonal cavities. Correspondingly, the room temperature Ge/Si photoluminescence was strongly enhanced, as evidenced by a $\times 30$ enhancement factor reported for a H2 cavity above $\lambda = 1.3 \mu\text{m}$. The combination of Ge/Si self-assembled islands with two-dimensional photonic crystals on SOI structures opens the route to the development of new silicon-based devices operating at the $1.55 \mu\text{m}$ telecommunication wavelength.

This work was supported by the Réseau Micro et Nano-Technologie (RMNT) under Contract No. 00V0091. The authors thank O. Kermarrec, Y. Campidelli, and D. Bensahel from STMicroelectronics for providing the silicon-on-insulator substrates.

- ¹S. Fan, P. R. Villeneuve, J. D. Joannopoulos, and E. F. Schubert, Phys. Rev. Lett. **78**, 3294 (1997).
- ²M. Boroditsky, T. F. Krauss, R. Coccioli, R. Vrijen, R. Bhat, and E. Yablonovitch, Appl. Phys. Lett. **75**, 1036 (1999).
- ³T. D. Happ, I. I. Tartakovskii, V. D. Kulakovskii, J.-P. Reithmaier, M. Kamp, and A. Forchel, Phys. Rev. B **66**, 041303(R) (2002).
- ⁴D. Labilloy, H. Benisty, C. Weisbuch, C. J. M. Smith, T. F. Krauss, R. Houdré, and U. Oesterle, Phys. Rev. B **59**, 1649 (1999).
- ⁵C. Reese, C. Becher, A. Imamoglu, E. Hu, B. D. Gerardot, and P. M. Petroff, Appl. Phys. Lett. **78**, 2279 (2001).
- ⁶T. Yoshie, A. Scherer, H. Chen, D. Huffaker, and D. Deppe, Appl. Phys. Lett. **79**, 114 (2001).
- ⁷M. Loncar, D. Nedeljkovic, T. P. Pearsall, J. Vuckovic, A. Scherer, S. Kuchinsky, and D. C. Allan, Appl. Phys. Lett. **80**, 1689 (2002).
- ⁸M. El kurdi, P. Boucaud, S. Sauvage, G. Fishman, O. Kermarrec, Y. Campidelli, D. Bensahel, G. Saint-Girons, I. Sagnes, and G. Patriarche, J. Appl. Phys. **92**, 1858 (2002).
- ⁹V. Le Thanh, V. Yam, P. Boucaud, F. Fortuna, C. Ulysse, D. Bouchier, L. Vervoort, and J. M. Lourtioz, Phys. Rev. B **60**, 5851 (1999).
- ¹⁰H. Benisty, C. Weisbuch, D. Labilloy, M. Rattier, C. J. M. Smith, T. F. Krauss, R. M. De la Rue, R. Houdré, U. Oesterle, C. Jouanin, and D. Cassagne, J. Lightwave Technol. **17**, 2063 (1999).
- ¹¹S. G. Johnson, P. R. Villeneuve, S. Fan, and J. D. Joannopoulos, Phys. Rev. B **62**, 8212 (2000).
- ¹²S. David, M. El kurdi, P. Boucaud, A. Chelnokov, V. Le Thanh, S. Sauvage, D. Bouchier, and J.-M. Lourtioz (unpublished).
- ¹³I. Alvarado-Rodriguez and E. Yablonovitch, J. Appl. Phys. **92**, 6399 (2002).